Polymer 50 (2009) 5456–5466

Contents lists available at ScienceDirect

Polymer

journal homepage: www.elsevier.com/locate/polymer

Comparison of the long range polymer chain dynamics of polystyrene and *cis*-polyisoprene using polymers randomly labeled with pyrene

Steven J. Teertstra, Wai Yau Lin, Mario Gauthier, Mark Ingratta, Jean Duhamel*

Institute for Polymer Research, Department of Chemistry, University of Waterloo, 200 University Avenue West, Waterloo, ON N2L 3G1, Canada

ARTICLE INFO

Article history:
Received 5 August 2009
Received in revised form
10 September 2009
Accepted 13 September 2009
Available online 17 September 2009

Keywords:
Fluorescence
Chain dynamics
Polyisoprene

ABSTRACT

The ability of the Fluorescence Blob Model (FBM) to probe the chain dynamics of a polymer backbone was verified for the first time by investigating whether it responds to known differences in backbone flexibility for flexible *cis*-polyisoprene (PIP) and more sterically hindered polystyrene (PS), both randomly labeled with pyrene. For comparable pyrene contents, the steady-state fluorescence spectra indicated that Py-PIP formed considerably more excimer than the Py-PS samples. Analysis of the fluorescence decays with the FBM provided the rate constant for intramolecular excimer formation. This rate constant was much larger for Py-PIP than for Py-PS, in agreement with the enhanced excimer formation observed for Py-PIP. The enhanced ability of Py-PIP to form excimer is attributed to the PIP backbone being less sterically hindered than the PS backbone. This study is the first example of a comparison of the long range polymer chain dynamics for two different polymeric backbones randomly labeled with pyrene.

© 2009 Elsevier Ltd. All rights reserved.

1. Introduction

Many properties of polymers in solution are affected by their chain dynamics. Examples of this include the time scale for the early collapse of an expanded polypeptide coil [1,2] or the dynamic exchange between the bridging and looping chains of associative thickeners that enables their gel to relax under shear [3,4]. Due to the wide range of polymer properties affected by chain dynamics, their study has been and continues to be the focus of sustained research. Experiments aiming at characterizing the chain dynamics of polymers in solution can be categorized into two major families depending on whether one monitors the time scale over which (1) a given unit of the chain loses its original orientation, or (2) two units of the chain encounter.

Experiments belonging to the first category include the measurement of the spin-lattice relaxation time T_1, spin-spin relaxation time T_2, and nuclear Overhauser enhancement (NOE) by ^{13}C or ^{15}N NMR spectroscopy [5], the analysis of ESR line shapes from spin-labeled polymers [6], or the measurement of the correlation time τ_c of a labeled polymer by fluorescence anisotropy [7]. These experiments reflect how quickly the initial orientation of the magnetic moment of a nucleus, the magnetic moment of an unpaired spinning electron, or the emission dipole moment of a chromophore are lost when monitored by NMR, ESR, and fluorescence spectroscopy, respectively. Earlier theoretical studies have established that these relaxation experiments reflect the dynamics of a few structural units located near the probe [8]. In other words, these experiments monitor local polymer chain dynamics.

Another family of experiments commonly used to characterize polymer chain dynamics is based on the covalent attachment of a chromophore and its quencher to a polymer, followed by the measurement of the rate at which the fluorescence of the excited chromophore is quenched. For reasons described in earlier reports [9,10], most of the fluorescence dynamic quenching (FDQ) experiments have been conducted on labeled polymers where the chromophore and the quencher were attached at the opposite ends of short, narrowly dispersed polymer chains [11–26]. Fewer experiments have been carried out with randomly labeled polymers [27–37] and among these, most quantitative analyses of the fluorescence decays have been performed with a semi-empirical Fluorescence Blob Model (FBM) [9,10,27,33–37]. In any case, whether the polymers are labeled at the chain ends or randomly along the chain, the FDQ experiments reflect the motions of the chromophore and quencher molecules separated by tens of structural units [9–37]. As a result, FDQ experiments probe long range polymer chain dynamics (LRPCD), although shortening the chain segment spanning the labels enables one to switch from LRPCD to local polymer chain dynamics [38–44].

The ultimate test to ensure the validity of experiments aiming at characterizing polymer chain dynamics consists in selecting two

* Corresponding author. Tel.: +1 519 888 4567; fax: +1 519 746 0435.
E-mail address: jduhamel@uwaterloo.ca (J. Duhamel).

0032-3861/$ – see front matter © 2009 Elsevier Ltd. All rights reserved.
doi:10.1016/j.polymer.2009.09.036

different polymeric backbones of known flexibility, applying the procedure of interest to probe polymer chain dynamics, and determining whether the procedure yields trends that reflect the known flexibility of the polymers. The ability of the NMR [5,45,46], ESR [6,47,48], fluorescence anisotropy relaxation [7,49–65], and end-to-end cyclization FDQ experiments [11–26] to probe chain dynamics has been validated for over 30 years. In particular, fluorescence anisotropy relaxation experiments conducted with anthracene-labeled polymers have established that polymer flexibility decreases in the sequence *cis*-polyisoprene > polystyrene > poly(α-methylstyrene) > poly(methyl methacrylate) [58,62]. End-to-end cyclization FDQ experiments have similarly established that polymer flexibility decreases in the sequence polydimethylsiloxane ≈ poly(tetramethylene oxide) > polystyrene [21]. In comparison, a much smaller number of FDQ experiments have been carried out with randomly labeled polymers. Most experiments with randomly labeled polymers have been conducted with pyrene-labeled polystyrene (Py-PS) [9,10,33–36] and poly(*N*,*N*-dimethylacrylamide) (Py-PDMA) [37]. Unfortunately, presumably due to their similar substituent bulkiness, no substantial differences in the FBM parameters describing their LRPCD were observed. These parameters include the size of a *blob*, N_{blob}, and the quenching rate constant inside a *blob*, k_{blob}. When the FBM analysis was applied to determine N_{blob} and k_{blob} for both polymers in a common solvent (*N*,*N*-dimethylformamide), these were found to equal 35 ± 3 and 0.8 $(\pm 0.1) \times 10^7\ s^{-1}$ for Py-PS [10] and 31 ± 3 and 1.1 $(\pm 0.1) \times 10^7\ s^{-1}$ for Py-PDMA [37], respectively. This result is reasonable considering that the characteristic ratio (C_∞) [66] and chain stiffness parameter (σ) [66] are similar for PS ($C_\infty \approx 10$, $\sigma = 2.22$) and PDMA ($C_\infty = 9.2$, $\sigma = 2.17$). In order to demonstrate that the FBM reliably reports on the LRPCD of a polymer backbone, it would be preferable to compare the trends obtained from the FBM analysis of two polymers of known and different flexibilities. To date, no study has been carried out with this specific purpose in mind.

The present study addresses this issue by comparing the trends obtained from the FBM analysis of the fluorescence decays acquired with pyrene-labeled *cis*-polyisoprene (PIP) and polystyrene (PS). These are good candidates for this purpose since fluorescence anisotropy relaxation experiments have established that PIP is substantially more flexible than PS [58,62]. The larger flexibility of PIP with respect to PS can also be inferred from C_∞ [66] and σ [67] which are both substantially larger for PS ($C_\infty \approx 10$, $\sigma = 2.22$) than for PIP ($C_\infty \approx 5$, $\sigma = 1.67$). The chromophore pyrene was selected to label the polymers due to its ability to form an excimer [68] upon encounter between an excited and a ground-state pyrene, also resulting in the quenching of the excited pyrene. Thus pyrene simplifies the synthetic procedure used to label the polymers since it acts as both the chromophore and its own quencher. Styrene can be copolymerized with an acrylate bearing a pyrene derivative to yield a pyrene-labeled PS (Py-PS), whereas a small fraction of the double bonds present in the PIP backbone can be modified to covalently attach pyrene and yield a pyrene-labeled PIP (Py-PIP). Since the attachment of bulky pyrene pendants hinders somewhat the mobility of the chain, a series of pyrene-labeled PS and PIP needed to be prepared with decreasing pyrene contents so that the parameters retrieved from the FBM analysis could be extrapolated to zero-pyrene content. Earlier studies have established that the extrapolated parameters describe properly the behavior of the naked polymer [27]. Furthermore, since earlier reports have established the sensitivity of the results derived from FBM analysis to the nature of the pyrene derivative used in the labeling reaction [69], special care was given to the design of the labeled constructs to ensure that the pyrene derivatives used had a similar chemical structure for the linker connecting the pyrene label to the polymer chains. The trends obtained with the FBM parameters extrapolated to zero-pyrene content for Py-PIP and Py-PS indicate that PIP is much more flexible than PS, in agreement with earlier reports using fluorescence anisotropy [58,62]. This report represents the first example in the literature where this comparison is based on FDQ experiments using randomly labeled polymers.

2. Experimental procedures

2.1. Reagent and solvent purification

Cyclohexane (BDH, HPLC grade) and toluene (BDH, HPLC grade) were purified by refluxing with oligostyryllithium under dry nitrogen (N_2) atmosphere. Tetrahydrofuran (THF; Caledon, reagent) was purified by distillation over triphenylmethylsodium under N_2. Isoprene (Aldrich, 99%) was purified by stirring and distillation over CaH_2 at atmospheric pressure, and was stored under N_2 at −20 °C until used. A second purification step was performed on a high-vacuum line immediately before polymerization by addition of *n*-butyllithium (*n*-BuLi; 2.5 M solution in hexane, 2.5 mL per 100 mL isoprene), degassing with three freezing-evacuation-thawing cycles, and condensation into an ampoule with a polytetrafluoroethylene stopcock. The initiator *sec*-butyllithium (*sec*-BuLi, Aldrich, 1.4 M solution in hexanes) was used as received. Its exact concentration was determined by the method of Burchat et al. [70] Pyridine was purified by distillation over CaH_2 at reduced pressure. 1-Pyrenebutyric acid (Aldrich, 97%) was purified by recrystallization from toluene. Anhydrous methanol was obtained by distillation over magnesium metal. *n*-Butyllithium (*n*-BuLi; Aldrich, 2.5 M solution in hexanes), 9-borabicyclo[3.3.1]nonane (9-BBN; Aldrich, 0.5 M solution in THF), hydrogen peroxide (BDH, 29-32% w/w), and oxalyl chloride (Aldrich, 98%) were used as received from the suppliers.

2.2. Synthesis of hydroxylated polyisoprene

Three linear polyisoprene samples with $M_w \approx 2500$, 10,000, and 30,000 g mol^{-1} were prepared in cyclohexane as described previously [71] to yield a microstructure with a high *cis*-1,4-isoprene units content. The polyisoprene samples were subjected to hydroboration according to a procedure outlined by Mao et al. [72] The hydroxylation of sample PIP30 ($M_w = 32{,}800$ g mol^{-1}, $M_w/M_n = 1.03$) is described here as an example: PIP30 (0.7 g, 10.3 mmol isoprene units) was dried under vacuum for 24 h before purification with three azeotropic distillation cycles using dry THF and dissolution in 25 mL of THF. A five-neck 500 mL glass reactor with a magnetic stirring bar was mounted on a high-vacuum line and fitted with the ampoule containing the purified linear polyisoprene, a dry THF inlet, a glass stopper, and a septum. The reactor was evacuated, flamed, and purged with purified N_2. THF (200 mL) was added to the flask along with the polymer solution, and the reactor was cooled to 0 °C. 9-BBN (7.2 mL, 6.16 mmol) was added with a syringe through the septum, and the reaction was allowed to proceed at 15 °C for 4 h. The solution was cooled to −30 °C and 1 mL of N_2-purged anhydrous methanol was added to quench excess 9-BBN. After 20 min, 1 mL of N_2-purged 6 M NaOH solution (1 mL, 6.16 mmol) was added. After 15 min N_2-purged H_2O_2 (2 mL, 6.16 mmol) was added dropwise over 5 min, which led to the formation of a white precipitate. The reaction was stirred for 1 h at −30 °C, warmed to room temperature over 30 min and maintained at that temperature for 2 h, and then warmed to 50 °C over 30 min and allowed to react further for 1 h. The solution was then cooled in a dry ice/2-propanol bath to freeze the aqueous phase containing the $NaB(OH)_4$ byproduct. The organic layer was added to 800 mL of 0.25 M NaOH solution and the precipitate formed was left to decant overnight. The polymer was collected, washed with distilled water,

redissolved in THF, and precipitated in a 0.25 M aqueous NaOH solution. Precipitation from THF into a 0.25 M aqueous NaOH solution was repeated twice, and a final time into a 1/1 methanol/distilled water mixture (v/v). The hydroxylated polyisoprene sample (PIP30-OH) was dried under vacuum for 72 h (yield 0.6 g, 15 mol% –OH groups).

2.3. Preparation of 1-pyrenebutyroyl chloride

1-Pyrenebutyric acid (2.0 g, 6.9 mmol) and toluene (20 mL) were combined under N_2 in a 100 mL round-bottomed flask fitted with a condenser. Oxalyl chloride (4.9 mL, 50 mmol) was added, and the mixture was stirred at room temperature for 30 min before refluxing for 3 h, by which time a homogeneous solution was obtained. The excess oxalyl chloride and the toluene were removed under vacuum, and 20 mL of freshly distilled toluene was added to the flask. Vacuum distillation of the toluene was repeated to remove residual oxalyl chloride, and 20 mL of freshly distilled toluene was added before the flask was sealed and stored in the dark. The resulting 1-pyrenebutyroyl chloride solution was used without product isolation in subsequent labeling reactions.

2.4. Pyrene-labeling of polyisoprene

The addition of incremental amounts of 1-pyrenebutyroyl chloride to the hydroxylated PIP substrates was performed in combination with sample removal from the reaction to obtain different labeling levels. The labeling reaction for sample PIP30 is described here as an example. PIP30-OH (0.62 g, 1.4 meq –OH groups) was dried for 2 h in a glass ampoule connected to a high vacuum line. The polymer was further purified by azeotropic distillation, using three cycles of dissolution and removal of anhydrous THF, before redissolution of the polymer in 10 mL of THF. Distilled pyridine (8 mL) was added and the solution was cooled to −30 °C. 1-Pyrenebutyroyl chloride solution (1.0 mL, ca. 0.35 mmol) was then added dropwise under vigorous stirring. The ampoule was warmed to room temperature, and the reaction was allowed to proceed for 1 h before a sample (5.0 mL) was removed. Cycles of reaction mixture cooling, acid chloride addition, and sampling were repeated six times to obtain labeled PIP samples (Py-PIP) with pyrene contents between 0.35 and 8.6 mol% based on the isoprene units.

2.5. Synthesis of (4-(1-pyrenyl)butyl)acrylate

The synthesis and purification of (4-(1-pyrenyl)butyl)acrylate (PyBA) has been described elsewhere [73]. A silica gel column using methylene chloride as eluent was used as an additional purification step to obtain the product as a colorless oil. Dissolution of the oil in ethyl acetate and hexane, followed by rotary evaporation of the solvent produced white crystals in 80% yield. 300 MHz ^{1}H NMR ($CDCl_3$) PyBA: δ 1.8–2.0 (m, 4H, $-CH_2-CH_2-$), δ 3.4 (t, 2H, $-CH_2$-Py), δ 4.2 (t, 2H, $-O-CH_2-$), δ 5.8 (d of d, 1H, alkene *trans*-H), δ 6.1 (q, 1H, alkene *gem*-H), δ 6.4 (d of d, 1H, alkene *cis*-H), δ 7.9–8.4 (m, 9H, pyrenyl H's).

2.6. Copolymerization

PyBA was copolymerized with styrene to generate a series of polystyrene samples randomly labeled with pyrene (Py-PS). The copolymerization was conducted according to a procedure reported earlier for the copolymerization of styrene with other pyrene-labeled monomers [69]. A conversion of less than 20% was used for all copolymerization reactions to minimize composition drift in the pyrene-labeled copolymers. The conversion was monitored during the reaction by ^{1}H NMR spectroscopy. The copolymer composition was also monitored as a function of conversion by injecting aliquots withdrawn from the copolymerization vessel into a GPC instrument equipped with an Agilent 1100 series fluorescence detector. The copolymer composition was considered to remain constant as long as no change in the excimer-to-monomer ratio was detected by the fluorescence detector. More details on this procedure can be found in an earlier publication [69].

2.7. Size exclusion chromatography

Absolute molecular weights for the PIP substrates were determined by size exclusion chromatography (SEC) analysis with a laser light scattering detector (SEC-LS). The Waters SEC system used consisted of an inline degasser (model AF), a 515 HPLC pump, a 717plus autosampler, a PLgel 10 μm guard column (Polymer Laboratories, 50 × 7.5 mm), and three HR 5E columns (Waters Associates, 300 × 7.5 mm, molecular weight range 2×10^3–4×10^6). THF at a flow rate of 1 mL/min served as the mobile phase. A Viscotek TDA 302 quad detector was used incorporating right-angle (RALS) and low-angle (LALS) light scattering detectors operating at 670 nm, differential refractometer (DRI), viscometer, and UV (model 2501) detectors. Molecular weights were obtained from the LALS and DRI signals using the OmniSEC v2.0 software package from Viscotek. The d*n*/d*c* values used in the SEC-LS measurements were determined using a Brice-Pheonix differential refractometer equipped with a 632 nm band-pass filter. Apparent molecular weights for Py-PIP and absolute molecular weights for Py-PS were determined by size exclusion chromatrography (SEC) using a linear polystyrene standards calibration curve and a DRI detector. The SEC system consisted of a Waters 590 HPLC pump, a Jordi 500 × 10 mm DVB linear mixed bed column (molecular weight range 10^2–10^7), and a Waters R401 DRI detector. THF at a flow rate of 1 mL/min served as the mobile phase.

2.8. ^{1}H NMR analysis

The PIP microstucture was determined by ^{1}H NMR analysis in $CDCl_3$ on a Bruker AC-300 nuclear magnetic resonance (NMR) spectrometer by established methods [74,75]. The hydroxylation level of the PIP-OH substrates was also determined by ^{1}H NMR analysis as previously reported [76].

2.9. UV-Vis absorption measurements

The pyrene content of the labeled polymers was determined by measuring the absorption for solutions of known concentrations of Py-PIP in THF and Py-PS in DMF using a Hewlett-Packard 8452A diode array spectrophotometer. The pyrene concentration [*Py*] of the solutions was estimated from the absorption at 344 nm and the molar absorption coefficient of 1-pyrenebutyric acid in THF (ε [344 nm, THF] = 41,500 $cm^{-1}\,M^{-1}$) or the averaged molar absorption coefficient of the model compounds 1−pyrenebutyric acid, 4−(1−pyrene)butylacrylamide, and 4−(1−pyrene)butylamine in DMF (ε [344 nm, DMF] = 37,200 ± 1000 $cm^{-1}\,M^{-1}$). The pyrene content (λ), expressed as moles of pyrene per gram of polymer, was calculated from

$$\lambda = \frac{[Py]V}{m} \tag{1}$$

where V is the volume of THF or DMF and m is the mass of polymer in the solution.

2.10. Steady-state and time-resolved fluorescence

The polymer solutions in THF (Caledon, distilled in glass) were purged with N_2 prior to acquiring the fluorescence spectra. The pyrene concentration was maintained at 3.0×10^{-6} M to avoid intermolecular excimer formation.

Steady-state fluorescence spectra were obtained with the usual right-angle configuration on a Photon Technology International LS-100 steady-state fluorometer with an Ushio UXL-75Xe Xenon arc lamp and a PTI 814 photomultiplier detection system. The samples were excited at 344 nm and the emission was monitored over the wavelength ranges 350–600 nm. The spectra were normalized at 375 nm, and the fluorescence intensities of the monomer (I_M) and the excimer (I_E) were calculated by integrating the spectra from 372–378 nm and 500–530 nm, respectively. The excimer intensity was measured above 500 nm to avoid overlap with the pyrene monomer emission.

Fluorescence decays were obtained by the time-correlated single-photon counting technique using a Photochemical Research Associates, Inc. System 2000 with a hydrogen lamp to excite the Py-PIP samples or an IBH time-resolved fluorometer fitted with an IBH 340 nm LED source to excite the Py-PS samples. The excitation wavelength was set at 344 nm, and the fluorescence of the pyrene monomer and excimer was monitored at 375 and 510 nm, respectively. Filters with cutoff wavelengths of 370 and 495 nm were used to block potential stray light scattering and to acquire the fluorescence decays for the pyrene monomer and excimer, respectively. All decays were collected over 512 channels for the Py-PIP samples and 1024 channels for the Py-PS samples, to a total of 20,000 counts at the peak maximum for the lamp and monomer decay curves, and a total of 10,000 counts for the excimer decay curves. The decay curves were analyzed using the δ-pulse deconvolution method [77]. Reference decay curves for N_2-purged solutions of PPO (2,5-diphenyloxazole) in cyclohexane ($\tau = 1.42$ ns) and BBOT (2,5-bis(5-*tert*-butyl-2-benzoxazolyl)thiophene) in ethanol ($\tau = 1.47$ ns) were used for the analysis of the monomer and excimer decay curves, respectively.

2.11. Analysis of fluorescence decays

Analysis of the fluorescence decays was carried out by convoluting the instrument response function $L(t)$ with a chosen function $f(t)$ used to fit the fluorescence decays according to Eq. (2).

$$F(t) = L(t) \otimes f(t) + a_{\text{scatt}} L(t) \tag{2}$$

The second term in Eq. (2) is a light scattering correction that accounts for processes occurring on a subnanosecond time scale, too fast to be detected by our time-resolved fluorometer. These rapid processes are believed to arise from the formation of excimer between two pyrenes covalently attached in close proximity along the polymer chain. The function $f(t)$ was either a sum of exponentials used to analyze the monomer and excimer decays or the FBM equation used to analyze the monomer fluorescence decays. Their expressions are given in Eqs. (3) and (4), respectively.

$$f(t) = \sum_{i=1}^{n} a_{X,i} \exp(-t/\tau_{X,i}) \quad \text{where } n = 2 \text{ or } 3 \text{ and}$$
$$X = M \text{ or } E \tag{3}$$

$$f(t) = f_{\text{Mdiff}} \exp\left[-\left(A_2 + \frac{1}{\tau_M}\right)t - A_3(1 - \exp(-A_4 t))\right] + f_{\text{Mfree}} \exp(-t/\tau_M) \tag{4}$$

The expressions for the parameters A_2, A_3, and A_4 in Equation (4) are given in Equation (5). These are expressed as a function of k_{blob}, $\langle n \rangle$, and $k_e[blob]$ which are, respectively, the rate constant associated with the encounter of an excited pyrene with a ground-state pyrene located inside the same *blob*, the average number of pyrenes per *blob*, and the product of the rate constant associated with the exchange of a ground-state pyrene from one *blob* to the next times the concentration of *blobs* within the polymer coil. The resulting function $F(t)$ in Equation (2) was compared with the experimental fluorescence decay, and the parameters used for the function $f(t)$ were optimized using the Marquardt–Levenberg algorithm [78].

$$A_2 = \langle n \rangle \frac{k_{\text{blob}} k_e[\text{blob}]}{k_{\text{blob}} + k_e[\text{blob}]}, \; A_3 = \langle n \rangle \frac{k_{\text{blob}}^2}{(k_{\text{blob}} + k_e[\text{blob}])^2},$$
$$A_4 = k_{\text{blob}} + k_e[\text{blob}] \tag{5}$$

According to the FBM the time-dependent behavior of the excited pyrene monomers is described by Equation (4), where f_{Mdiff} refers to the fraction of pyrene monomers able to form excimer by diffusion and $f_{\text{Mfree}} = 1 - f_{\text{Mdiff}}$ refers to the fraction of pyrenes bound to the polymer that do not form excimer and fluoresce as unattached or free pyrene monomers with their natural lifetime τ_M.

2.12. Error analysis

To test the reliability of FBM analysis of the fluorescence decays, the parameters f_{Mdiff}, f_{Mfree}, k_{blob}, k_{ex}, and $\langle n \rangle$ retrieved from each analysis based on Eqs. (4) and (5) were used to generate a set of 20 simulated decays, each having a different pattern of Poisson noise. The 20 simulated decays were then analyzed to yield 20 sets of f_{Mdiff}, f_{Mfree}, k_{blob}, k_{ex}, and $\langle n \rangle$ values which were used to determine average values (m) and standard deviations (δ). The percentage deviation from the average value (δ/m) was always below 0.01, 0.02, 0.05, 0.05, and 0.02 for f_{Mdiff}, f_{Mfree}, k_{blob}, k_{ex}, and $\langle n \rangle$, respectively.

3. Results and discussion

Earlier reports have established that different trends are obtained from FBM analysis of the fluorescence decays acquired for the same polymer backbone labeled with different pyrene derivatives [69]. Consequently, special attention was paid to the labeling procedure used in the current investigation. The chemical structure of the Py-PS and Py-PIP samples is compared in Table 1. The pyrene pendants were connected to the polymer chain via a 6-atom linker in the Py-PS samples. Depending on whether 1-pyrenebutyroyl chloride reacted with hydroxylated 1,4-, 1,2-, or 3,4-isoprene units, the length of the spacer in Py-PIP varied between 5–7 atoms. For both polymeric constructs, a flexible ester bond served to covalently attach the pyrene derivatives. Furthermore, the 1-pyrenebutyl moiety present in both the Py-PIP and Py-PS constructs ensured that the lifetime of the pyrene label in THF was the same ($\tau_M = 210$ ns), providing the same probing time for both polymers. This is an important point to consider, since the *blob* size retrieved from FBM analysis of the fluorescence decays depends strongly on the lifetime of the fluorescent probe [79–81]. Whereas the Py-PS samples were prepared by a straightforward copolymerization reaction similar to those conducted earlier with other pyrene-labeled polystyrenes [69], the Py-PIP samples used a "grafting onto" procedure.

The characteristics of the PIP substrates are summarized in Table 2. The three polymers ($M_w \approx 2500$, 10,000, and 30,000 g mol^{-1}) were prepared by anionic polymerization in cyclohexane, yielding a narrow molecular weight distribution ($M_w/M_n \leq 1.11$) and

Table 1
Chemical Structure of the Pyrene-labeled Polymers.

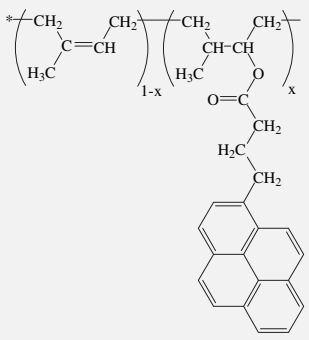

Pyrene-labeled polyisoprene: Py-PIP (1-pyrenebutyroyl label attached to a 1,4-isoprene unit is shown)

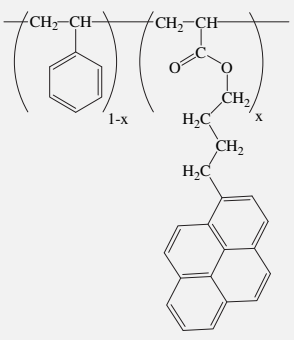

Pyrene-labeled polystyrene: Py-PS

a microstucture with a high proportion (~70 mol%) of *cis*-1,4-isoprene units. The PIP substrates were subjected to hydroboration and oxidation reactions to introduce hydroxyl groups on about 15% of the structural units along the polymer chains. The rigorous purification protocol reported by Mao et al. [72] was applied to ensure complete removal of the boric acid byproduct, known to cause cross-linking in hydroxylated PIP [73]. The PIP-OH samples retained a low apparent polydispersity index after modification by hydroboration ($M_w/M_n^{app} = 1.13$, 1.09, and 1.08 for PIP2.5-OH, PIP10-OH, and PIP30-OH, respectively), as determined by SEC analysis using a calibration curve based on linear polystyrene standards (Figure SI.1).

Attachment of the pyrene labels to PIP-OH was achieved by coupling 1-pyrenebutyroyl chloride with the pendent hydroxyl functionalities along the PIP backbone. The acyl chloride was prepared from oxalyl chloride and 1-pyrenebutyric acid, and used without purification in the labeling reactions after the removal of excess oxalyl chloride under vacuum. Incremental additions of 1-pyrenebutyroyl chloride and samples removal yielded a series of PIP with identical molecular weights but different labeling levels from a single reaction. The acyl chloride was added at low temperature with vigorous stirring to promote a more uniform distribution of pyrene labels along the polymer chains. ^{1}H NMR spectra are compared in Figure SI.2 for a linear polyisoprene substrate (PIP2.5, $M_w \approx 2500$ g mol^{-1}), a hydroxylated polyisoprene (PIP2.5-OH, 13 mol% –OH groups), and a pyrene-labeled polymer (Py-PIP2.5, 9.9 mol% pyrene). Following hydroxylation, the doublet for the olefinic protons of the 3,4-isoprene units at 4.7 ppm disappeared, and additional peaks were observed with chemical shifts assigned as follows: hydroxyl protons (4.5 ppm), [–CH_2–CH(CH(CH_3)–CH_2(OH))–] and [–CH_2–CH(OH)–CH(CH_3)–CH_2–] (3.4–3.6 ppm), [–CH_2–CH(CH(CH_3)–CH_2(OH))–] and [–CH_2–CH(OH)–CH(CH_3)–CH_2–] (0.8 ppm). The terminal alkene of 3,4-isoprene units is most reactive toward hydroboration [82], reacting completely to give 6 mol% of hydroxyl groups in all the polyisoprene samples. The reaction of the more hindered 1,4-isoprene units was much slower, resulting in the balance of the hydroxyl substitution. It is impossible to determine whether the *cis*- or *trans*-1,4-isoprene units reacted preferentially due to peak overlap in the ^{1}H NMR spectra. Following the reaction of the hydroxylated polymer with pyrenebutyroyl chloride, new peaks appeared in the ^{1}H NMR spectra due to the bound pyrene moieties, with chemical shifts assigned as follows: pyrene aromatic protons (7.7–8.4 ppm), [–C(=O)–CH_2–CH_2–CH_2–Py] (3.3 ppm), [–C(=O)–CH_2–CH_2–CH_2–Py] (2.4 ppm), [–CH_2–CH(CH(CH_3)–CH_2(O–C(=O)–(CH_2)$_3$–Py))–] (3.8–4.1 ppm) and [–CH_2–C***H***(O–C(–O)–(CH_2)$_3$–Py)–CH(CH_3)–CH_2–] (4.9 ppm).

The labeling reaction is relatively free of side reactions, as the polydispersity of the Py-PIP samples remained low (PDI = $M_w/M_n \leq 1.13$). A series of SEC traces provided in Figure SI.1 illustrates the evolution of the molecular weight distribution in the synthesis of a Py-PIP10 sample with 7.9 mol% pyrene. The PDI values for the Py-PS samples (about 1.65) obtained by free radical copolymerization, given in Table 3 together with the pyrene contents and the M_n values, are much larger than for the Py-PIP samples. However large PDI values have been shown not to affect the FBM parameters describing the LRPCD of a polymeric backbone [36]. This result is a consequence of the principle by which the FBM operates. By characterizing the LRPCD of the chain segment located inside a *blob* instead of the LRPCD of the entire chain, the FBM is not affected by effects due to differences in chain length or polydispersity, as long as the chain is longer than a *critical polymer chain length* (*cpcl*) found to be between 5000 and 40,000 g mol^{-1} for PS [36].

The pyrene content of the labeled polymers can be described either by the percentage of pyrene-labeled structural units in the chain ($\lambda_{\%}$) expressed in mol%, the molar fraction of pyrene-labeled structural units in the chain ($x = \lambda_{\%}/100$), the number of moles of pyrene per gram of polymer (λ_{Py}), or the percentage of carbon atoms in the backbone bearing a pyrene groups ($\lambda_{\%}^C = \lambda_{\%}/4$ and $\lambda_{\%}/2$ for the Py-PIP and Py-PS samples, respectively). Five different pyrene contents ranging from $\lambda_{\%} = 1.6$ to 8.1 mol% were obtained for each series of pyrene-labeled polymer.

The units used to express the polymer chain length (degree of polymerization, DP) need to be discussed since the isoprene and styrene structural units do not have the same number of carbon atoms: Consequently, a chain incorporating 50 styrene units is 100 carbon atoms long, while a chain with 50 isoprene units is 200 carbon atoms long (assuming a predominantly 1,4-microstructure as in the present case). To account for this difference and in agreement with earlier studies [11,18], the trends obtained for the parameters describing the LRPCD of PS and PIP will be discussed in terms of the number of carbon atoms making up a chain using $\lambda_{\%}^C$ as a scaling parameter in all instances unless otherwise noted.

Steady-state fluorescence spectra were recorded for each pyrene-labeled polymer at a pyrene concentration of 3.0×10^{-6} M, as determined by UV absorption analysis. This concentration is low enough to prevent intermolecular excimer formation [83]. The steady-state fluorescence spectra acquired for the Py-PIP30 and Py-PS samples in THF are provided in Fig. 1A and B, respectively. The spectra were normalized at 375 nm, corresponding to the 0 – 0

Table 2
Characterization Data for *cis*-1-4-polyisoprene substrates.

Polymer	M_n^{LSa}	M_w/M_n^{LSa}	PIP Microstructure[b]/mol%			OH[b]/mol%
			cis-1,4-	*trans*-1,4-	3,4-	
PIP2.5	2290[c]	1.11	69	25	6	13
PIP10	9380	1.02	71	23	6	15
PIP30	32,800	1.03	72	22	6	15

[a] Absolute M_n determined from SEC-LS.
[b] Microstructure and hydroxylation level determined by ^{1}H NMR analysis.
[c] M_n from ^{1}H NMR analysis.

Table 3
Characterization Data for the Py-PS series.

$\lambda_{\%}$ mol% pyrene	$\lambda_{\%}^C$ mol% pyrene	$\lambda_{Py} \times 10^{-4}$ mol g^{-1}	M_n kg mol^{-1}	M_w/M_n
2.1	1.05	1.9	46	1.65
3.1	1.55	2.8	43	1.67
4.5	2.25	3.9	49	1.62
5.4	2.70	4.7	53	1.69
6.0	3.00	5.1	46	1.68

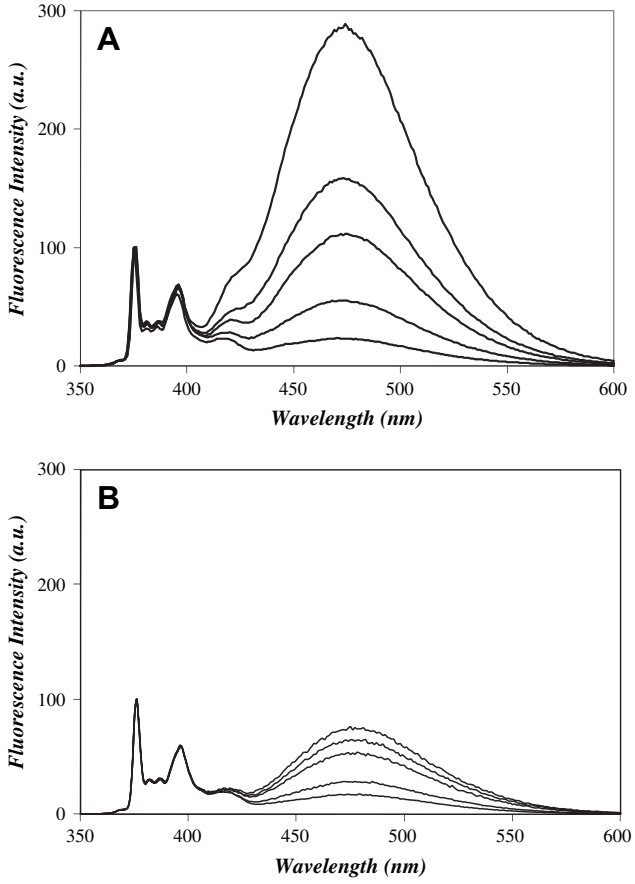

Fig. 1. Steady-state fluorescence spectra of the pyrene-labeled polymers in THF. (A): Py-PIP30 with pyrene contents (from bottom to top) of 1.6, 2.7, 4.3, 5.9, and 8.1 mol%. B): Py-PS with pyrene contents (from bottom to top) of 2.1, 3.1, 4.5, 5.4, and 6.0 mol%. $[Py] = 3.0 \times 10^{-6}$ M; $\lambda_{ex} = 344$ nm.

peak. For each sample series, increasing the pyrene content of the polymer enhances the number of pyrene-pyrene encounters and leads to more efficient excimer formation. More importantly, excimer formation appears to be much higher for Py-PIP (Fig. 1A) than for Py-PS (Fig. 1B), suggesting enhanced flexibility of the PIP backbone. However this effect could also be attributed to differences in local concentration of pyrene labels within the polymer coils.

To confirm the origin of this difference, the ratio of the fluorescence intensity of the excimer over that of the monomer (I_E/I_M) was determined for each pyrene-labeled polymer and plotted in Fig. 2 as a function of the pyrene content ($\lambda_{\%}^{C}$). The identical I_E/I_M trends observed for the Py-PIP10 and Py-PIP30 samples indicate that the I_E/I_M ratio does not depend on polymer chain length, as long as the polymer chain length is greater than the *cpcl*, which apparently corresponds to a molecular weight between 2500 and 10,000 g mol^{-1} for PIP. This observation for narrowly dispersed PIP samples mirrors that made about 10 years ago for narrowly dispersed PS samples, for which a *cpcl* between 5000 and 40,000 g mol^{-1} was determined [36]. The overlapping I_E/I_M data for PIP10 and PIP30 in Fig. 2 suggest that excimer formation occurs locally in the polymer coil within a subdomain having a size that is independent of the overall molecular weight of the PIP chains. The diverging I_E/I_M trend observed for Py-PIP2.5 indicates that the size of the subdomain becomes comparable to or larger than that of the polymer coil of PIP2.5. The overlap observed between the I_E/I_M trends obtained for PIP10-Py and PIP30-Py demonstrates that for these polymers, with a chain length larger than the *cpcl*, the I_E/I_M ratio becomes insensitive to chain length. Consequently, no additional experiments were undertaken with chains longer than the PIP30 sample.

Interestingly, the Py-PS samples yielded much lower I_E/I_M ratios (Fig. 2) than all the Py-PIP samples, still reflecting the trends shown in Fig. 1. An expression derived by Perico and Cuniberti [28] for the I_E/I_M ratio of polymers randomly labeled with pyrene is given by the equation:

$$\frac{I_E}{I_M} = \kappa \frac{\phi_E^o}{\phi_M^o} \tau_M k_1 [Py]_{loc} \tag{6}$$

The parameters κ, τ_M, ϕ_E^o, and ϕ_E^o in Eq. (6) represent, respectively, a constant that accounts for the geometry and the sensitivity of the spectrofluorometer used, the lifetime of the pyrene monomer, the fluorescence quantum yield of the monomer, and that of the excimer. The parameter κ does not change for the Py-PIP and Py-PS samples, since all experiments were conducted on the same steady-state fluorometer. Since the same 1-pyrenebutyl moiety was used for both the Py-PIP and Py-PS samples (Table 1), the parameters τ_M, ϕ_M^o, and ϕ_E^o should likewise be unaffected. Thus the I_E/I_M ratio is expected to depend uniquely on k_1, the bimolecular encounter rate constant between an excited and a ground-state pyrene bound to the chain, and $[Py]_{loc}$, the effective concentration of the ground-state pyrenes in the neighborhood of an excited pyrene.

The I_E/I_M ratios obtained for Py-PIP in Fig. 2 are at least 3 times larger than those obtained for Py-PS over the whole composition ($\lambda_{\%}^{C}$) range investigated. Therefore if $[Py]_{loc}$ is the same for Py-PS and Py-PIP, these results indicate that k_1 in Eq. (6) is about three times larger for PIP than for PS. The local concentration $[Py]_{loc}$ should at least be the same when comparing PIP and PS samples with identical numbers of pyrenes per chain and hydrodynamic volumes. The hydrodynamic volume of PIP30, estimated from its intrinsic viscosity in THF at 25 °C ($[\eta] = 0.38$ dL g^{-1}), is $V_h = 830$ nm^3. The molecular weight M of a PS chain having the same V_h as the PIP chain, estimated by combining the Einstein and Mark–Houwink–Sakurada (MHS) equations, is $M = (2.5\, N_A\, V_h/K)^{1/1+\alpha}$ with N_A = Avogadro's number, $K = 0.011$ mL g^{-1}, and $\alpha = 0.725$ for PS in THF at 25 °C [66]. The PS equivalent molecular weight obtained by this method is 47,000 g mol^{-1}, also (coincidentally) corresponding to the average M_n measured for the Py-PS copolymer series synthesized (Table 3). Most importantly, this equivalent PS sample has a molecular weight above the known *cpcl* value of polystyrene (5000–40,000 g mol^{-1}). Since a 30 K PIP chain occupies the same

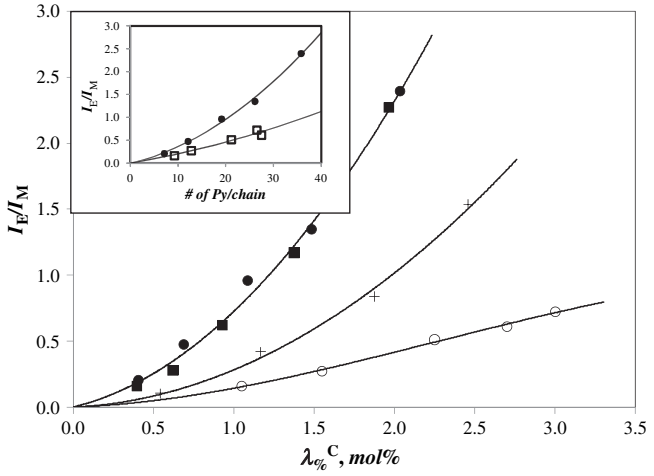

Fig. 2. Ratio I_E/I_M in THF as a function of pyrene content for PIP2.5-Py (+), PIP10-Py (■), PIP30-Py (●), and Py-PS (○). Inset: I_E/I_M as a function of the number of pyrenes per chain for PIP30-Py and Py-PS. $[Py] = 3.0 \times 10^{-6}$ M; $\lambda_{ex} = 344$ nm.

Table 4
Parameters Retrieved from the Fits of the Pyrene Excimer Fluorescence Decays of Py-PIP and Py-PS in THF with a Sum of Exponentials.

	Py mol/%	τ_{E1} (ns)	$a_{E1}/(a_{E3}+a_{E4})$	τ_{E2} (ns)	$a_{E2}/(a_{E3}+a_{E4})$	τ_{E3} (ns)	$a_{E3}/(a_{E3}+a_{E4})$	τ_{E4} (ns)	$a_{E4}/(a_{E3}+a_{E4})$	χ^2
PIP2.5[a]	4.8	17	−0.71			61	1.0			1.13
	7.6	13	−0.62			60	1.0			1.22
	9.9	8.2	−0.68			57	1.0			1.16
PIP10	1.6	19	−0.74			72	0.91	140	0.09	1.05
	2.5	21	−0.77			71	0.93	140	0.07	1.06
	3.7	16	−0.70			65	0.99	150	0.01	1.08
	5.5	11	−0.71			58	1.0			1.19
	7.9	8.9	−0.53			53	1.0			1.14
PIP30	1.6	20	−0.73			73	0.92	140	0.08	1.17
	2.7	17	−0.76			68	0.98	140	0.02	1.17
	4.3	14	−0.74			60	1.0			1.08
	5.9	12	−0.70			56	1.0			1.07
	8.1	7.4	−0.63			51	1.0			1.05
PS	2.1	13	−0.19	36	−0.76	68	0.77	121	0.23	1.13
	3.1	9	−0.16	29	−0.79	71	0.87	115	0.13	1.00
	4.5	6	−0.14	23	−0.82	7	1.00			1.16
	5.4	9	−0.22	24	−0.72	65	1.00			1.16
	6.0	7	−0.19	23	−0.76	64	1.00			1.10

[a] Only the Py-PIP samples with the higher pyrene contents generated enough excimer to acquire a fluorescence decay.

hydrodynamic volume as a 47 K PS chain, the I_E/I_M ratio for the PIP30-Py and Py-PS samples was plotted as a function of the number of pyrenes per chain in the inset of Fig. 2. The trend obtained for the Py-PS sample in the inset of Fig. 2 is therefore representative of the behavior of PS chains with a hydrodynamic volume equivalent to that of PIP30-Py, and consequently a comparable local concentration of pyrene within the polymer coils. Since the I_E/I_M ratio for the PIP30-Py series remains much larger than the I_E/I_M ratio for the Py-PS series, this observation leads to the conclusion that k_1 in Eq. (6) is indeed much larger for PIP than for PS, reflecting the enhanced flexibility of the PIP backbone.

Fluorescence decays were acquired at 375 and 510 nm for the pyrene monomer and excimer, respectively, by exciting the solutions with the pyrene-labeled polymers in THF at 344 nm. The excimer decays were fitted with two to four exponentials according to Eq. (3). The decay times and pre-exponential factors obtained from this analysis are listed in Table 4. The decay times τ_{E1} and τ_{E2} represent the rise time associated with negative pre-exponential factors whereas the decay times τ_{E3} and τ_{E4} represent the decaying part of the curve, associated with positive pre-exponential factors. Of particular interest is the ratio a_{E-}/a_{E+} for the sum of the negative pre-exponential factors over the sum of the positive pre-exponential factors. An a_{E-}/a_{E+} ratio equal to −1.0 indicates that excimer formation occurs by diffusive encounters only, whereas a more positive value suggests that some pyrenes are close to each other and form excimer on a subnanosecond time scale that cannot be probed by the instrument [9,27,36,69].

The a_{E-}/a_{E+} ratios were -0.69 ± 0.07 and -0.95 ± 0.01 for the Py-PIP and Py-PS samples, respectively. In analogy to other investigations, the samples where pyrene was incorporated via copolymerization (Py-PS) yielded a_{E-}/a_{E+} ratios substantially closer to −1.0 than the samples where pyrene was grafted onto the polymer (Py-PIP) [69,84]. A less negative a_{E-}/a_{E+} ratio suggests that the pyrene pendants are somewhat clustered in the case of the Py-PIP samples, which in turn could affect the parameters retrieved from the FBM analysis. Furthermore, it should be pointed out that a_{E-}/a_{E+} ratios similar to those obtained for Py-PIP were obtained when 1-pyrenemethoxide was reacted with a chloromethylated PS substrate in a grafting-onto reaction to yield GrE-PS [69]. A more negative a_{E-}/a_{E+} ratio was obtained when pyrene was incorporated into a PS

Table 5
Parameters Retrieved from the FBM Analysis of the Pyrene Monomer Fluorescence Decays of the Py-PIP and Py-PS Samples in THF.

	Py mol/%	$\lambda_{Py} \times 10^{-4}$ mol/g	f_{Mdiff}	f_{Mfree}	k_{blob} (10^7 s^{-1})	$k_e[blob]$ (10^6 s^{-1})	$\langle n \rangle$	χ^2
PIP2.5	2.1	2.9	0.52	0.48	4.9	1.5	1.1	1.35
	4.8	5.9	0.78	0.22	3.8	1.1	1.7	1.10
	7.6	8.4	0.91	0.09	4.0	0.8	2.3	1.11
	9.9	10.2	0.97	0.03	4.1	0.6	2.8	1.07
PIP10	1.6	2.2	0.75	0.25	2.3	6.5	1.2	0.98
	2.3	3.1	0.79	0.21	2.6	6.3	1.4	1.01
	3.7	4.7	0.96	0.05	2.4	5.5	1.9	0.99
	5.5	6.6	0.98	0.02	2.9	6.3	2.5	1.01
	7.9	8.7	0.99	0.01	3.8	6.3	3.3	0.98
PIP30	1.6	2.2	0.87	0.13	2.1	6.0	1.1	1.17
	2.7	3.6	0.97	0.03	2.2	5.4	1.6	1.19
	4.3	5.4	0.99	0.01	2.3	5.5	2.4	1.08
	5.9	7.0	0.99	0.01	3.0	6.7	2.7	1.03
	8.1	8.9	0.99	0.01	3.5	5.9	3.6	0.96
PS	2.1	1.9	0.94	0.06	1.0	4.3	1.1	1.01
	3.1	2.8	0.98	0.02	1.2	4.5	1.5	1.18
	4.5	3.9	0.99	0.01	1.4	6.1	2.1	1.21
	5.4	4.7	0.99	0.01	1.5	6.8	2.3	1.26
	6.0	5.1	0.99	0.01	1.6	7.2	2.4	1.06

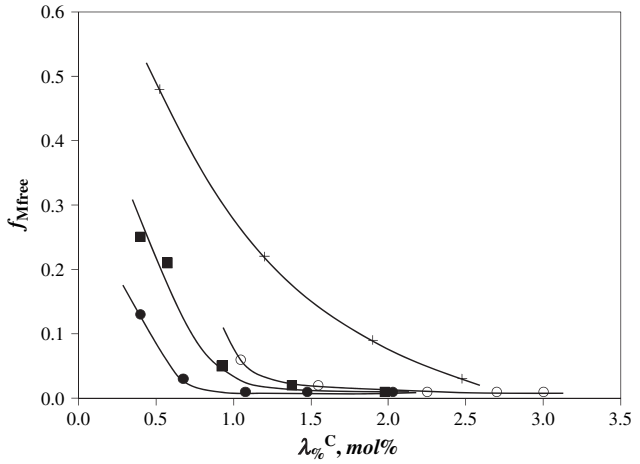

Fig. 3. f_{Mfree} as a function of pyrene content for PIP2.5-Py (+), PIP10-Py (■), PIP30-Py (●), and Py-PS (○). $[Py] = 3.0 \times 10^{-6}$ M; $\lambda_{ex} = 344$ nm.

backbone by copolymerizing 4-(1-pyrenyl)methoxymethylstyrene with styrene to yield CoE-PS [69]. Although GrE-PS and CoE-PS had the same chemical structure, the pyrene pendants were more clustered on GrE-PS than CoE-PS. Yet the parameters derived from FBM analysis of the fluorescence decays acquired for GrE-PS and CoE-PS were comparable [69]. Consequently, the more positive a_{E-}/a_{E+} ratios observed for the Py-PIP samples are not expected to have negative consequences on the parameters retrieved from the FBM analysis conducted hereafter.

The monomer decays were fitted with Eq. (4). The pyrene monomer lifetimes τ_M determined in the analysis of Py-PIP and Py-PS were 200 and 210 ns, respectively. These values were determined by fitting the fluorescence decay of Py-PIP and Py-PS samples having a pyrene content of less than 0.4 mol% with a sum of three exponentials (Eq. (3) with $n = 3$). The low pyrene content of these samples ensured that little excimer was formed, so that the long component of the decay could be assigned unambiguously to the natural lifetime for the emission of unquenched excited 1-pyrenebutyl pendants attached to PIP (200 ns) and PS (210 nm). These τ_M values compare favorably with the lifetime of 207 ns measured for 1-pyrenebutyric acid in THF at a concentration of 2.4×10^{-6} M. The fit for the monomer fluorescence decays with Eq. (4) yielded the parameters f_{Mdiff}, k_{blob}, $\langle n \rangle$, and $k_e[blob]$ which are listed in Table 5 with the χ^2 values. The fits yielded χ^2 values below 1.20 in all but one case, and the residuals as well as the autocorrelation function of the residuals were randomly distributed around zero, indicating good quality fits.

Quenching of an excited pyrene by styrene units has been reported in one instance [85]. The rate constant of quenching of pyrene by an atactic polystyrene was found to equal 1.75×10^5 M^{-1} s^{-1} monomer^{-1} in THF. Based on the MHS parameters for PS in THF used earlier [66], the Py-PS samples used in this study exhibit a local styrene concentration of ~ 1 mol L^{-1} assuming a molecular weight of 47,000 g mol^{-1} and a hydrodynamic volume of 830 nm^3. Consequently, the rate constant of quenching of an excited pyrene by nearby styrene monomers is much smaller ($< 0.2 \times 10^6$ s^{-1}) than the k_{blob} and $k_e[blob]$ values reported in Table 5. Thus the rate at which an excited pyrene is quenched by a nearby styrene via either exciplex formation or electron transfer is expected to be negligible compared to the rate of excimer formation, as described by the parameters k_{blob} and $k_e[blob]$.

The parameter f_{Mdiff} denotes the fraction of pyrene groups forming excimer by diffusion, whose emission is described by the FBM. The fraction of pyrenes which do not form excimer is $f_{Mfree} = 1 - f_{Mdiff}$ and represents the chromophores located in pyrene-deficient domains of the polymer coil, emitting as if they were unattached or free. The f_{Mfree} values for the Py-PIP10 and Py-PIP30 samples and all Py-PS samples were less than 0.1 for $\lambda_{\%}^{C}$ values larger than 1.0 mol%. Fig. 3 represents the f_{Mfree} values of all pyrene-labeled polymers as a function of $\lambda_{\%}^{C}$. In all cases f_{Mfree} decreases with increasing pyrene content, reflecting an increase in $[Py]_{loc}$ and the associated enhancement in excimer formation by diffusive encounters. Interestingly, the trend for the Py-PIP2.5 samples stands out because it yields much larger f_{Mfree} values than all other samples. This indicates that the Py-PIP2.5 samples have a much larger fraction of pyrene monomers that do not form excimer. A possible reason for this could be the small size of Py-PIP2.5, which favors the isolation of pyrene labels on different chains. The substantial fraction of pyrene monomers that do not form excimer in Py-PIP2.5 also explains why the I_E/I_M ratios for Py-PIP2.5 in Fig. 2 were always lower than those obtained for Py-PIP10 and Py-PIP30.

Figs. 4 and 5 provide the rate constant k_{blob} and the number of carbon atoms encompassed in a chain segment defining a *blob*, N_{blob}^{C}. Whereas k_{blob} is obtained directly by fitting the pyrene monomer fluorescence decay curves with Eq. (4), N_{blob}^{C} is calculated from the parameters $\langle n \rangle$ and f_{Mdiff} according to Equation (7), where M_{Py} and M_{mono} are the molar masses of the pyrene-labeled structural units (M_{Py} equals 356 and 328 g mol^{-1} for Py-PIP and Py-PS) and the unlabeled structural units (M_{mono} equals 104 and 68 g mol^{-1} for styrene and isoprene), respectively. The parameter n^C represents the number of carbon atoms from each structural unit becoming incorporated into the polymer backbone, equaling 2 and 4 for styrene and isoprene, respectively. The molar fraction of pyrene labeled monomers is represented by x.

$$N_{blob}^{C} = n^{C} \times \frac{\langle n \rangle}{\lambda_{Py}/f_{Mdiff}\left[M_{Py}(x) + M_{mono}(1-x)\right]} \tag{7}$$

As often determined in FBM studies, k_{blob} and N_{blob}^{C} respectively increase and decrease for increasing pyrene contents [9,27,36,69]. These trends are internally consistent. Indeed, k_{blob} is a pseudo-unimolecular rate constant that is expected to equal the product of the bimolecular rate constant, k_1^{blob}, describing the diffusive encounters between two pyrenes attached to the polymer, and the local concentration equivalent to one pyrene inside a *blob*, $1/V_{blob}$, where V_{blob} is the volume of a *blob* [9,37,69]. This relationship is shown in Eq. (8). Similar equations have been derived to describe the quenching of a chromophore by a quencher located inside a surfactant micelle [86] or at the opposite ends of narrowly dispersed polymer chains [15,87]. Assuming that k_1^{blob} does not change with the pyrene content for a given polymer, an increase in k_{blob} with increasing pyrene content indicates a decrease in V_{blob}

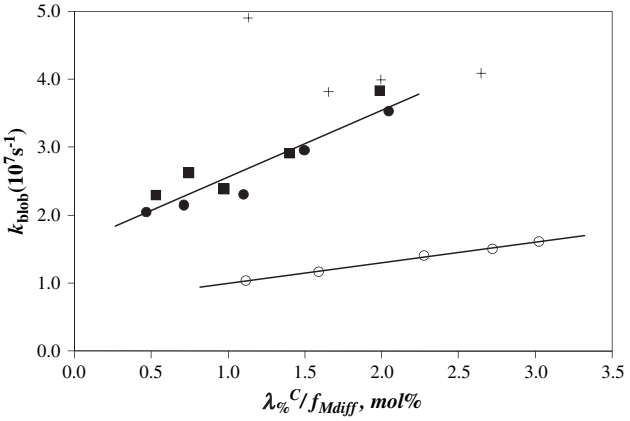

Fig. 4. Plot of k_{blob} versus $\lambda_{\%}^{C}/f_{Mdiff}$ for PIP2.5-Py (+), PIP10-Py (■), PIP30-Py (●), and Py-PS (○).

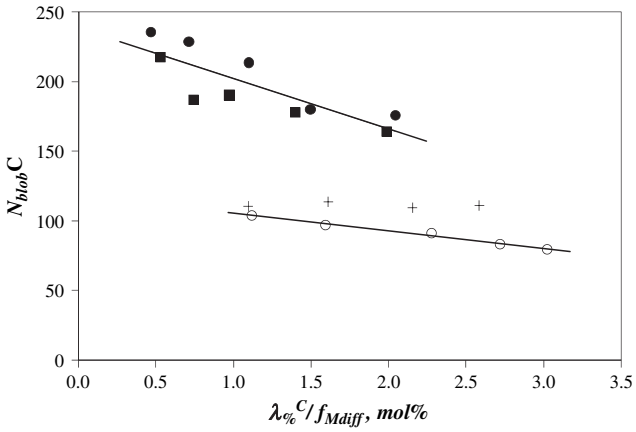

Fig. 5. Plot of N_{blob}^{C} versus $\lambda_{\%}^{C}/f_{Mdiff}$ for PIP2.5-Py (+), PIP10-Py (■), PIP30-Py (●), and Py-PS (○).

and N_{blob}^{C}. This decrease in V_{blob} has been attributed to a decrease in the mobility of the polymer chain as an increasing number of bulky pyrene pendants are attached to the chain [9,27,36,69]. The values of k_{blob}^{o} and $N_{blob}^{C,o}$ describing an ideal PIP and PS *blob* (i.e. a *blob* with no pyrene attached to the polymer) can be obtained by extrapolating the trends in Figs. 4 and 5 to zero pyrene content [9,27,36,69]. Extrapolation of the trends yields $k_{blob}^{o} = 1.4(\pm 0.2) \times 10^{7}\ s^{-1}$ and $N_{blob}^{C,o} = 244(\pm 12)$ for PIP, and $k_{blob}^{o} = 0.7(\pm 0.1) \times 10^{7}\ s^{-1}$ and $N_{blob}^{C,o} = 120(\pm 2)$ for PS.

$$k_{blob} = k_{1}^{blob} \times \frac{1}{V_{blob}} \tag{8}$$

In terms of the number of structural units per *blob* (N_{blob}), a PIP *blob* made of 244 ± 12 carbon atoms contains 61 ± 3 structural units, the same size as a PS *blob* made of 120 ± 2 carbon atoms or 60 ± 1 structural units. Nevertheless, $N_{blob}^{C,o}$ for PIP being twice larger than for PS suggests that the volume V_{blob} probed by an excited pyrene is larger for PIP than for PS. According to Eq. (8), this observation should result in a smaller k_{blob}^{o} value for PIP; yet the opposite trend is observed with k_{blob}^{o} being twice larger for PIP than for PS. A logical conclusion on the basis of these results is that excimer formation is facilitated for Py-PIP, in agreement with the I_E/I_M trends shown in Fig. 2. While each isoprene unit in PIP incorporated a rigid double bond, the rotation of the single bonds on either side of the double bond is relatively unhindered. The situation is different for PS where a bulky phenyl substituent on every second carbon atom hinders chain rotation. A similar decrease in chain mobility has also been inferred when monitoring the correlation time of anthracene covalently attached to PIP or PS by fluorescence anisotropy measurements [58,62].

An $N_{blob}^{C,o}$ value of 244 carbon atoms represents a PIP segment weighing $M_{blob}^{o} = 4.2\ kg\ mol^{-1}$; so the polymer coils of PIP10 and PIP30 incorporate on average 2.4 and 7.2 *blobs*, respectively. Figs. 4 and 5 yield similar trends for k_{blob} and N_{blob}^{C} derived from the Py-PIP and Py-PS samples. On the other hand PIP2.5, which has an M_n value smaller than M_{blob}^{o}, yields k_{blob} and N_{blob}^{C} trends that diverge from those obtained for PIP10 and PIP30. Also M_{blob}^{o} for PIP2.5 is only 1.9 kg mol^{-1}, different from the M_{blob}^{o} value retrieved for PIP10 and PIP30.

Earlier studies have shown that the product $k_{blob} \times N_{blob}$ (or $k_{blob} \times N_{blob}\langle n \rangle/\lambda_{\%}^{C}$) is a measure of the rate constant for intramolecular excimer formation, and as such reflects the LRPCD of a polymer [9,10]. Consequently, the product $k_{blob} \times N_{blob}^{C}$ could serve to compare the dynamics of different polymer chains, as long as similar fluorescent derivatives are used to label the polymers being compared as it was done in the present study (Table 1). The product $k_{blob} \times N_{blob}^{C}$ was plotted as a function of $\lambda_{\%}^{C}$ in Fig. 6. Interestingly, although k_{blob} in Fig. 4 and N_{blob}^{C} in Fig. 5 for the Py-PIP2.5 samples are very different from the values obtained for Py-PIP10 and Py-PIP30, the product $k_{blob} \times N_{blob}^{C}$ for Py-PIP2.5 ($470\ (\pm 50) \times 10^{7}\ s^{-1}$) is close to that obtained for Py-PIP10 and Py-PIP30 ($520\ (\pm 60) \times 10^{7}\ s^{-1}$). Since these experiments probe the same type of polymer (PIP), this observation suggests that even if different k_{blob} and N_{blob}^{C} parameters are obtained for a same polymer due to differences in polymer chain length, the product $k_{blob} \times N_{blob}^{C}$ is useful as a general measure of the LRPCD of a polymer.

The data shown in Fig. 6 indicate that on average, $k_{blob} \times N_{blob}^{C}$ for Py-PIP is about 4.2 (±0.9) times larger than for Py-PS. On the basis of earlier reports suggesting that $k_{blob} \times N_{blob}^{C}$ provides a reliable measure of LRPCD [9,10], the result in Fig. 6 implies that PIP is much more flexible than PS. It must be pointed out that this conclusion is not affected even if the number of structural units per *blob* (N_{blob}^{o}) is considered instead of $N_{blob}^{C,o}$. Since Py-PIP and Py-PS yield the same N_{blob}^{o} of about 60 structural units (*vide supra*) but k_{blob}^{o} is twice larger for Py-PIP than for Py-PS, the product $k_{blob} \times N_{blob}$ is twice larger for Py-PIP than for Py-PS. This conclusion is in agreement with the less sterically hindered structure of PIP relatively to PS, as well as the shorter average correlation time obtained when the chromophore anthracene is covalently attached to PIP than to PS [58,62].

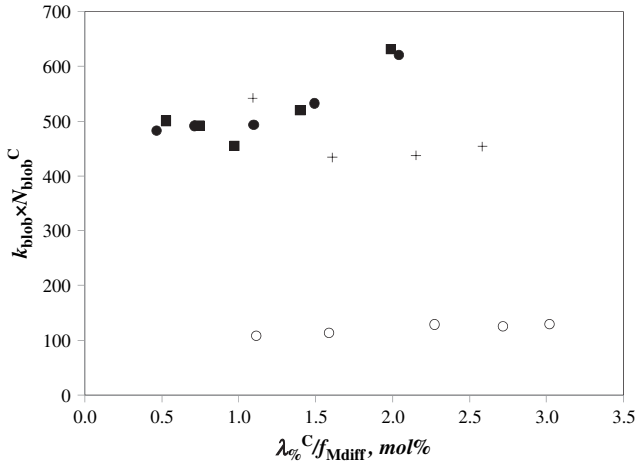

Fig. 6. Plot of $k_{blob} \times N_{blob}^{C}$ versus $\lambda_{\%}^{C}/f_{Mdiff}$ for PIP2.5-Py (+), PIP10-Py (■), PIP30-Py (●), and Py-PS (○).

4. Conclusions

The LRPCD of two polymeric backbones have been compared in FDQ experiments. *cis*-Polyisoprene and polystyrene were randomly labeled with a 1-pyrenebutyl derivative, to achieve spacing of the pyrene labels from the backbone chain by about the same number of atoms (5–7) in both systems. Furthermore, an ester bond was used to link pyrene to the backbone in both cases. Consequently, the lifetime of the pyrene moieties in both constructs was similar and found to equal 200 ns and 210 ns for Py-PIP and Py-PS, respectively. These considerations of the length and nature of the linker, and the pyrene lifetime are important, since variations in these parameters can lead to noticeable differences in the trends obtained in FDQ experiments [69]. Similar pyrene derivatives ensure that the trends obtained for the different polymers accurately reflect their LRPCD and are not due to differences in characteristics of the pyrene labels.

PIP was labeled with pyrene by hydroxylating ~ 15% of the double bonds and coupling the hydroxyl groups with 1-

pyrenebutyroyl chloride. The Py-PS samples were obtained by copolymerization of small amounts of 4-(1-pyrenyl)butylacrylate with styrene. The process of excimer formation was monitored by steady-state and time-resolved fluorescence for the Py-PS and Py-PIP samples. All the fluorescence measurements conducted in this study consistently indicated that Py-PIP forms excimer much more efficiently than Py-PS. The I_E/I_M ratios for the Py-PIP samples were much larger than for the Py-PS samples. The product $k_{blob} \times N^C_{blob}$, characterizing the rate constant of intramolecular excimer formation, was found to be ~4 times larger for Py-PIP than for Py-PS. Enhanced excimer formation in Py-PIP can be rationalized by the unhindered rotation of the methylene units along the PIP backbone. In comparison, rotation around the PS backbone is hindered by the bulky benzene ring borne by each styrene structural unit. These conclusions are in agreement with those drawn from fluorescence anisotropy experiments [58,62]. This study represents the first example in the literature where fluorescence data obtained for two different polymers randomly labeled with pyrene were analyzed quantitatively to compare their LRPCD.

The existence of a *critical polymer chain length* (*cpcl*), suggested 10 years ago in a study of a series of pyrene-labeled narrowly dispersed polystyrenes, was also confirmed for the Py-PIP samples. All the trends observed in Figs. 1–5 for Py-PIP2.5 were very different from those obtained for the Py-PIP10 and Py-PIP30 samples. The difference in the behavior of the Py-PIP2.5 samples is attributed to the unit size of a *blob*, found to be 61 isoprene structural units, larger than the 27 isoprene structural units constituting PIP2.5. The shorter Py-PIP2.5 chains resulted in the isolation of a large fraction of the pyrene labels (Fig. 3). Although the data obtained with Py-PIP2.5 do not scale in the same manner as those obtained with Py-PIP10 and Py-PIP30, the product $k_{blob} \times N^C_{blob}$ yielded similar values irrespective of whether it was obtained with the Py-PIP2.5 samples or the longer ones. This result suggests that $k_{blob} \times N^C_{blob}$ reflects the LRPCD of a given backbone, regardless of whether the polymer studied has a chain length that is shorter or longer than that encompassed inside a *blob*.

Acknowledgements

This study would not have been possible without the financial support of NSERC.

Appendix. Supplementary data

SEC profiles of the PIP10 sample at each step of the labeling procedure. ^{1}H NMR spectra acquired at each step of the labeling procedure for the PIP2.5 sample. Supplementary data associated with this article can be found in the online version, at doi:10.1016/j.polymer.2009.09.036.

References

[1] Eaton WA, Muñoz V, Hagen SJ, Jas GS, Lapidus LJ, Henry ER, et al. Annu Rev Biophys Biomol Struct 2000;29:327–59.
[2] Bilsel O, Matthews CR. Curr Opin Struct Biol 2006;16:86–93.
[3] Winnik MA, Yekta A. Curr Opin Colloid Interface Sci 1997;2:424–36.
[4] Tripathi A, Tam KC, McKinley GH. Macromolecules 2006;39:1981–99.
[5] Daragan VA, Mayo KH. Prog Nucl Magn Reson Spectrosc 1997;31:63–105.
[6] Pilař J. In: Schlick S, editor. Advanced ESR methods in polymer research. Hoboken: Wiley-Interscience; 2006.
[7] Viovy J-L, Monnerie L. Adv Polym Sci 1985;67:99–122.
[8] Valeur B, Jarry J-P, Geny F, Monnerie L. J Polym Sci: Polym Phys Ed 1975; 13:667–74.
[9] Ingratta M, Hollinger J, Duhamel J. J Am Chem Soc 2008;130:9420–8.
[10] Ingratta M, Duhamel J. Macromolecules 2009;42:1244–51.
[11] Winnik MA. Acc Chem Res 1985;18:73–9.
[12] Pandey S, Kane MA, Baker GA, Bright FV, Fürstner A, Seidel G, et al. J Phys Chem B 2002;106:1820–32.
[13] Gardinier WE, Kane MA, Bright FV. J Phys Chem B 2004;108:18520–9.
[14] Gardinier WE, Bright FV. J Phys Chem B 2005;109:14824–9.
[15] Cuniberti C, Perico A. Eur Polym J 1977;13:369–74.
[16] Cheung S-T, Winnik MA, Redpath AEC. Makromol Chem 1982;183:1815–24.
[17] Winnik MA, Redpath T, Richards DH. Macromolecules 1980;13:328–35.
[18] Svirskaya P, Danhelka J, Redpath AEC, Winnik MA. Polymer 1983;24:319–22.
[19] Redpath AEC, Winnik MA. J Am Chem Soc 1982;104:5604–7.
[20] Winnik MA, Redpath AEC, Paton K, Danhelka J. Polymer 1984;25:91–9.
[21] Slomkowski S, Winnik MA. Macromolecules 1986;19:500–1.
[22] Xu H, Martinho JMG, Winnik MA, Beinert G. Makrom Chem 1989;190: 1333–43.
[23] Farinha JPS, Martinho JMG, Xu H, Winnik MA, Quirk RP. J Polym Sci Part B Polym Phys 1994;32:1635–42.
[24] Martinho JMG, Reis e Sousa AT, Winnik MA. Macromolecules 1993;26:4484–8.
[25] Reis e Sousa AT, Castanheira EMS, Fedorov A, Martinho JMG. J Phys Chem A 1998;102:6406–11.
[26] Farinha JPS, Piçarra S, Miesel K, Martinho JMG. J Phys Chem B 2001;105: 10536–45.
[27] Duhamel J. Acc Chem Res 2006;39:953–60.
[28] Cuniberti C, Perico A. Eur Polym J 1980;16:887–93.
[29] Winnik MA, Egan LS, Tencer M, Croucher MD. Polymer 1987;28:1553–60.
[30] Wang FW, Lowry RE. Polymer 1985;26:1046–52.
[31] Seixas de Melo J, Costa T, Miguel MG, Lindman B, Schillen K. J Phys Chem B 2003;107:12605–21.
[32] Seixas de Melo J, Costa T, Francisco A, Maçanita AL, Gago S, Gonçalves IS. Phys Chem Chem Phys 2007;9:1370–85.
[33] Picarra S, Relogio P, Afonso CAM, Martinho JMG, Farinha JPS. Macromolecules 2003;36:8119–29.
[34] Picarra S, Relogio P, Afonso CAM, Martinho JMG, Farinha JPS. Macromolecules 2004;37. 1670–1670.
[35] Picarra S, Duhamel J, Fedorov A, Martinho JMG. J Phys Chem B 2004;108: 12009–15.
[36] Mathew H, Siu H, Duhamel J. Macromolecules 1999;32:7100–8.
[37] Kanagalingam S, Ngan CF, Duhamel J. Macromolecules 2002;35:8560–70.
[38] Kanaya T, Goshiki K, Yamamoto M, Nishijima Y. J Am Chem Soc 1982;104: 3580–7.
[39] Almeida LM, Vaz WLC, Zachariasse KA, Madeira VMC. Biochemistry 1982;21: 5972–7.
[40] Zachariasse KA, Duveneck G, Busse R. J Am Chem Soc 1984;106:1045–51.
[41] Zachariasse KA, Duveneck G. J Am Chem Soc 1987;109:3790–2.
[42] Reynders P, Kühnle W, Zachariasse KA. J Am Chem Soc 1990;112:3929–39.
[43] Zachariasse KA, Maçanita AL, Kühnle W. J Phys Chem B 1999;103:9356–65.
[44] Liao T-P, Morawetz H. Macromolecules 1980;13:1228–33.
[45] Waldow DA, Johnson BS, Hyde PD, Ediger MD, Kitano T, Ito K. Macromolecules 1989;22:1345–51.
[46] Glowinkowski S, Gisser DJ, Ediger MD. Macromolecules 1990;23:3520–30.
[47] Pilař J, Labský J, Marek A, Budil DE, Earle KA, Freed JH. Macromolecules 2000;33:4438–44.
[48] Pilař J, Labský J. Macromolecules 2003;36:913–20.
[49] Kasparyan-Tardiveau N, Valeur B, Monnerie L, Mita I. Polym 1983;24:205–8.
[50] Valeur B, Monnerie L, Jarry J-P. J Polym Sci: Polym Phys Ed 1975;13:675–82.
[51] Valeur B, Monnerie L. J Polym Sci: Polym Phys Ed 1976;14:11–27.
[52] Valeur B, Monnerie L. J Polym Sci: Polym Phys Ed 1976;14:29–37.
[53] Viovy JL, Monnerie L, Brochon JC. Macromolecules 1983;16:1845–52.
[54] Veissier V, Viovy J-L, Monnerie L. Polymer 1989;30:1262–8.
[55] Waldow DA, Ediger MD, Yamaguchi Y, Matsushita Y, Noda I. Macromolecules 1991;24:3147–53.
[56] Adolf DB, Ediger MD, Kitano TT, Ito K. Macromolecules 1992;25:867–72.
[57] Horinaka J-I, Aoki H, Ito S. Yamamoto M. Polym J 1999;31:172–6.
[58] Ono K, Ueda K, Yamamoto M. Polym J 1994;26:1345–51.
[59] Ono K, Okada Y, Yokotsuka S, Sasaki T, Yamamoto M. Macromolecules 1994;27:6482–6.
[60] Ono K, Sasaki T, Yamamoto M, Yamasaki Y, Ute K, Hatada K. Macromolecules 1995;28:5012–6.
[61] Tsunomori F, Ushiki H. Polym J 1996;28:576–81.
[62] Ono K, Ueda K, Sasaki T, Murase S, Yamamoto M. Macromolecules 1996;29: 1584–8.
[63] Horinaka J-I, Amamno S, Funada H, Ito S, Yamamoto M. Macromolecules 1998; 31:1197–201.
[64] Horinaka J-I, Maruta M, Ito S, Yamamoto M. Macromolecules 1999;32:1134–9.
[65] Aoki H, Horinaka J-I, Ito S, Yamamoto M, Katayama H, Kamigaito M, et al. Polym J 2001;33:464–8.
[66] Bandrup J, Immergut EH, Grulke EA. Polymer handbook. 4th ed. New York: Wiley; 1999. p. VII 23.
[67] Boyer RF, Miller RL. Macromolecules 1977;10:1167–8.
[68] Birks JB. Photophysics of aromatic molecules. New York: Wiley; 1970. p. 301.
[69] Ingratta M, Duhamel J. Macromolecules 2007;40:6647–57.
[70] Burchat AF, Chong JM, Nielsen N. J Organomet Chem 1997;542:281–3.
[71] Kee RA, Gauthier M. Macromolecules 1999;32:6478.
[72] Mao G, Wang J, Clingman SR, Ober CK, Chen JT, Thomas EL. Macromolecules 1997;30:2556.
[73] Ge Z, Luo S, Liu S. J Polym Sci Part A: Polym Chem 2006;44:1357–71.

[74] Essel A, Pham QT. J Polym Sci Part A-1: Polym Chem 1972;10:2793.
[75] Tanaka Y, Takeuchi Y, Kobayashi M, Tadokoro H. J Polym Sci Part A-2: Polym Phys 1971;9:43.
[76] Lee KM, Han CD. Macromolecules 2002;35:760.
[77] Demas JN. Excited-state lifetime measurements. New York: Academic; 1983. p. 102.
[78] Press WH, Flannery BP, Teukolsky SA, Vetterling WT. Numerical recipes. The art of scientific computing (fortran version). Cambridge: Cambridge University; 1992. p. 523.
[79] Kanagalingam S, Spartalis J, Cao T-C, Duhamel J. Macromolecules 2002;35:8571–7.
[80] Ingratta M, Duhamel J. J Phys Chem B 2008;112:9209–18.
[81] Ingratta M, Duhamel J. J Phys Chem B 2009;113:2284–92.
[82] Chung TC, Raate M, Berluche RE, Schulz DN. Macromolecules 1988;21:1903.
[83] Kim SD, Torkelson JM. Macromolecules 2002;35:5943–52.
[84] Duhamel J, Kanagalingam S, O'Brien T, Ingratta M. J Am Chem Soc 2003;125:12810–22.
[85] Redpath AEC, Pekcan O, Winnik MA. J Photochem 1983;23:283–8.
[86] Almgren M, Löfroth J- E. J Colloid Interface Sci 1981;81:486–99.
[87] Cuniberti C, Perico A. Prog Polym Sci 1984;10:271–316.